Mansoura University
Faculty of Engineering
Mansoura Engineering Journal

Modeling of Carbon Dioxide Capture in Fluidized Bed

نموذج رياضي لإجراء فصل ثاني أكسيد الكربون في المهد المميع

Shady Emad*, Ahmed A. Hegazi, Salah H. El-Emam and Farouk M. Okasha

KEYWORDS:
Carbon Capture, Global Warming, Calcium Looping, Fluidized Bed

الملخص العربي:- أدى التزايد المستمر في حرق الوقود الحفري إلى زيادة معدل انبعاثات ثاني أكسيد الكربون مما تسبب بدوره في تفاقم مشكلة الاحتباس الحراري. ويعتبر امتصاص ثاني أكسيد الكربون من غازات العادم وتخزينه ضمن الحلول المقترحة للحد من تلك الانبعاثات. وتشير العديد من الأبحاث والدراسات البيئية إلى إمكانية تحقيق ذلك عن طريق استخدام حبيبات أكسيد الكالسيوم عبر تفاعلها مع ثاني أكسيد الكربون لتكوين كربونات الكالسيوم فيما يسمى بتفاعل الكربنة. ويقدم هذا البحث نموذج رياضي لعملية كربنة أكسيد الكالسيوم في مهد مميع. وقد تم التحقق من صحة نتائج هذا النموذج عن طريق مقارنتها ببعض النتائج التي تم الحصول عليها معمليا في معمل الاحتراق بجامعة المنصورة وأيضا بنتائج نظرية لآخرين. تم استخدام النموذج الرياضي لمعرفة تأثير عوامل التشغيل المختلفة على كفاءة امتصاص ثاني اكسيد الكربون حيث وجد أن أقصى كفاءة تحدث عند قرابة الـ 675 درجة مئوية. كما لوحظ أن تقليل سرعة التمييع وزيادة حجم الحبيبات لهما تأثير متشابه في تحسين انتقال الكتلة وزيادة الزمن المتاح لإتمام عملية الكربنة مما يزيد من كفاءة امتصاص ثاني اكسيد الكربون. وقد توافقت هذه النتائج بشكل كبير مع النتائج المنشورة في أبحاث سابقة. وجد أيضا أن كفاءة الامتصاص تزداد تدريجيا بزيادة ارتفاع المهد إلى حد معين ، حيث لا تتأثر كفاءة الامتصاص بشكل واضح بأي زيادة أخرى في ارتفاع المهد. وتفيد النتائج التي تم التوصل إليها إلى إمكانية استخدام النموذج الرياضي المقترح كأداة تصميمية في اختيار ظروف التشغيل التي تحقق تحسين امتصاص ثاني أكسيد الكربون من عوادم الاحتراق تمهيدا لتسويقها تجاريا وتطبيقها على المستوى الصناعي.

***Abstract*— Carbon capture and storage (CCS) has been globally gaining popularity as a viable greenhouse gases mitigation strategy throughout the last decade. Calcium looping (CaL) is an emerging technology to capture carbon dioxide from flue gases of fossil fueled power plants exploiting the reversible gas-solid reaction between the carbon dioxide (CO2) and calcium oxide (CaO) to form calcium carbonate (CaCO3) in a fluidized bed. In this work, a dynamic model of a bubbling bed carbonator, the key reactor in the capture process, has been presented. The model incorporate both hydrodynamics and chemical kinetics to provide more reliable predictions. The model has been validated with experimental data obtained at combustion lab, Mansoura University using a fluidized bed carbonator of 10.5 cm inner diameter as well as a mathematical model found in literature. The key parameters have been investigated to check for system sensitivity. Bed temperature has a non-monotonic effect on CO2 capture efficiency. Maximum CO2 capture efficiency was found to occur around a temperature of 675 °C. Capture efficiency increases with either decreasing fluidization velocity or increasing bed particle size due to enhanced mass transfer and increased residence time. These findings almost accord with published data. Also, the average CO2 capture efficiency was found to increase with increasing static bed height up to a certain limit. Further increase in bed height doesn't considerably affect the capture efficiency. The proposed model can be used as a design tool that would enable the optimization and commercialization of calcium looping.**

Received: 29 September, 2016 - accepted: 2 November, 2016
Shady Emad, Mechanical Power Engineering Department, Faculty of Engineering,
Mansoura University, El-Mansoura, 35516, Egypt
Email : shadyemad@mans.edu.eg

I. INTRODUCTION

GLOBAL warming has many consequences including sea water level increase, agriculture and fisheries disruption, atmospheric warming, and prevalence of different diseases such as malaria. Global warming is mainly caused by anthropogenic emissions of so

called greenhouse gases (mainly carbon dioxide (CO_2)). The burning of fossil fuels, including coal, oil, and gas constitutes the major source of CO_2 emissions. Fossil fuel-based emissions of CO_2 may be originated from both stationary (e.g., power plant) and non-stationary systems (e.g., automobile). However, power generation sector is responsible for the largest amounts of CO_2 emissions. Due to the dependence on fossil fuels to meet more than 85% of the world's energy needs, the scientific community agrees that the solution for mitigating CO_2 emissions for the short- to midterm lies in a portfolio of strategies, including carbon capture and storage [1].

Carbon capture and storage, or CCS, is a family of technologies and techniques that enables the capture of CO_2 from fuel combustion or industrial processes, the transport of captured CO_2 via ships or pipelines, and its storage underground, in depleted oil and gas fields and deep saline aquifer formations. CCS can have a unique and vital role to play in the global transition to a sustainable low-carbon economy, in both power generation and industry. An overview of different CCS technologies can be found in [2,3]. The most critical step in the CCS chain that determines the feasibility of a certain technique is the capture step [1].

One of the promising technologies that has shown some potential advantages in terms of net efficiency and cost of CO_2 avoided on both lab and pilot scale is carbon dioxide capture by absorption/regeneration process with calcium oxide, known as calcium looping as shown in Fig. 1. Both the carbonation and calcination reactions are carried out at high temperatures (600–700 $°C$) and (900–950 $°C$) respectively, allowing for efficient heat recovery in heating process or steam cycle of a power generation system.

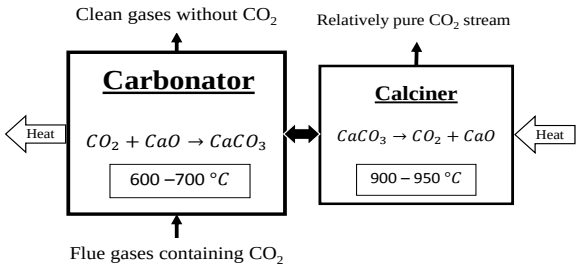

Fig. 1 Calcium looping process

Hirama et al. [4] patented separation of carbon dioxide from gases containing it by contacting the gas mixture with metal based oxides (e.g. calcium oxide) to form metal carbonate. The metal oxide is then regenerated at higher temperatures in a second contacting zone where heat is supplied. The application of CaL as a post-combustion CO_2 capture process with dual fluidized bed was then proposed by Shimizu et al. [5]. Since then, a lot of research has been done to further analyze and develop the process [6–8]. Moreover, several projects have been established to assess its feasibility on both lab and pilot scales [9–12].

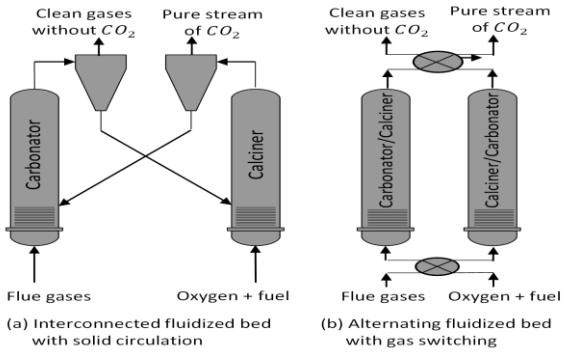

Fig. 2 Dual fluidized bed configurations

Figure 2 shows two different dual fluidized bed configurations that can be used in the calcium looping process where heat is supplied in the calciner by oxyfuel combustion. Most research works have focused on the interconnected fluidized bed with solids circulation between carbonator and calciner, Fig. 2a. However, the present work has been dedicated to study the mode of alternating bed with gas switching, Fig. 2b. It consists of two separate fluidized beds (e.g. bubbling-bubbling) where carbonation and calcination reactions take place periodically in each reactor.

In the alternating bed configuration, flue gases are admitted to the carbonator where calcium oxide particles capture carbon dioxide from the gases mixture. When almost CaO particles get converted into $CaCO_3$ (i.e. the bed is no longer capable of capturing CO_2), supplying flue gases is stopped and fuel with oxygen is admitted (oxyfuel combustion) to provide heat and operate the reactor as a calciner. During calcination, a relatively pure stream of CO_2 is released and can be further compressed and transported for geological sequestration.After CaO is regenerated in the calciner, carbonation starts again and the cycle is repeated periodically. To allow continuous capture, dual alternating fluidized beds are used with gas switching between them.

In the present study, a mathematical model for a bubbling bed reactor operating in carbonation mode, where capturing of CO_2 takes place, is developed. The fluidization phenomenon is studied and its effects on mass transfer between different phases and residence time of gas molecules in the reactor are investigated. The model pays due attention to the kinetic parameters controlling the reaction rate and its dependence on operating conditions (e.g. operating temperature and CO_2 partial pressure). Model calculations yield axial concentration profiles of carbon dioxide in the bed phases. Model predictions are compared with data found in literature. Parametric study is carried out to explore the key parameters that affect the capture process.

II. MODEL DESCRIPTION

2.1 Kinetic Model

Carbon capture in carbonator takes place through the exothermic reaction of calcium oxide with carbon dioxide as follows:

$$CaO + CO_2 \rightarrow CaCO_3 \quad (1)$$

As can be seen from Eq. (1), the carbonation reaction is a non-catalytic heterogeneous gas-solid reaction and there exists an equilibrium partial pressure of carbon dioxide depending on the operating conditions. Baker [13] proposed an equation where operating temperature is the only independent variable as follows;

$$\log_{10} P_{eq}(atm) = 7.079 - \frac{38000}{4.574 * T} \quad (2)$$

This heterogeneous carbonation reaction is characterized by an initial fast stage controlled by chemical kinetics at reaction surface followed by a much slower stage controlled by diffusion of gas through the product layer of calcium carbonate. In most industrial applications, the diffusion stage is commonly neglected and calcium oxide is considered to reach its maximum conversion at the end of the kinetically controlled stage.

The formation of the product layer prevents the unreacted core from contacting the reacting gas which requires the gas to diffuse through this product layer to reach the core. Furthermore, the formation and growth of solid product affects the porous structure by filling the pores, decreasing the available surface area for reaction.

The thickness of this product layer formed on the free surface of CaO is a critical parameter to mark the end of the fast reaction period. Many researchers investigated the average value for the critical $CaCO_3$ product layer thickness [14]. The theory of a critical product layer thickness has been used almost exclusively to explain the "maximum" conversion during carbonation reaction cycles giving acceptable results [15,16], however these works lack the important effect of operating temperature on chemical kinetics. They consider that operating temperature only determines the equilibrium partial pressure of carbon dioxide. However, experiments indicate greater role for temperature in the reaction scenario [17].

The grain model for porous solids [18] is adopted here to model the gas-solid reaction between CO_2 and CaO.

The reaction rate for a gas–solid reaction is usually

$$R = \frac{dX}{dt(1-X)} \quad (3)$$

Defined as a specific reaction rate R, where;

When the reaction is under kinetic control, the specific rate can be further expressed in power law form [19];

$$R = 56\, k_s.\left(P_{CO_2} - P_{CO_2,eq}\right)^n.S \quad (4)$$

Assuming that reaction takes place uniformly on spherical grains, the following equation can be used,

$$1 - X = \left(\frac{r}{r_0}\right)^3 \quad (5)$$

Combining Eqs. (3), (4) and (5) would result in:

$$\frac{dX}{dt} = 56\, k_s.S_0.\left(P_{CO_2} - P_{CO_2,eq}\right)^n.(1-X)^{\frac{5}{3}} \quad (6)$$

Sun et al. [19] reported a first-order reaction changing to zero-order dependence when the CO_2 partial pressure exceeded 10 kPa.

The kinetic constant can be evaluated using Arrhenius equation;

$$k_s = k_0\,.\exp\left(-\frac{E}{R_u.T}\right) \quad (7)$$

Kinetic parameters (k_0 *and* E) are obtained from experimental measurements and values reported by Sun et al. [19] are adopted here.

Barker [20] reported that the carbonation reaction, presented by Eq. (1), is far from reversible in practice. The sorption capacity in the fast reaction stage decreases rapidly with increasing the number of calcination–carbonation cycles. Grasa and Abanades [21] proposed the semi-empirical equation (15) to express the sorbent capacity after a large number of complete carbonation–calcination cycles (up to500). It is valid for different sorbents and for a wide range of operating conditions.

$$X_{max,N} = \frac{1}{\frac{1}{(1-X_r)} + k.N} + X_r \quad (8)$$

Where k and X_r represent the deactivation constant and the residual conversion, respectively. It is observed that values of $k = 0.52$ and $X_r = 0.075$ fit well with a wide range of sorbents and conditions [21].

2.2 Hydrodynamic Model

Kunii-Levenspiel model for bubbling bed is widely accepted for its simplicity and reliable results [22]. A bubbling fluidized bed consists mainly of two phases, bubbles and emulsion. Bubbles are lean phase free of solid particles, while emulsion is a dense phase where solid particles are assumed to be uniformly distributed.

Minimum Fluidization:

The minimum fluidization velocity, u_{mf}, is calculated using the correlation proposed by Wen and Yu [23] as

$$Re_{p,mf} = \frac{\rho_g.d_p.u_{mf}}{\mu} = \sqrt{C_1^2 + C_2.Ar} - C_1 \quad (9)$$

follows;

Where: $Ar = \frac{d_p^3.\rho_g.(\rho_s-\rho_g).g}{\mu^2}$

C_1 and $C_2$are constants with values of 27.2 and 0.0408, respectively as suggested by Grace [24].

The porosity at the minimum fluidization conditions ε_{mf} is calculated with the expression proposed by Broadhurst and Becker [25], where;

$$\varepsilon_{mf} = 0.586\,\phi^{-0.72}Ar^{-0.029}\left(\frac{\rho_g}{\rho_s}\right)^{0.021} \quad (10)$$

Emulsion Phase:

The emulsion phase is assumed to be at minimum fluidization condition. Hence, the superficial rise velocity of emulsion gas is considered to be the same as (u_{mf}).

Bubble Phase:

Bubble Size

Bubbles size can be estimated using the traditional Darton's correlation [26] where,

$$d_b = 0.54\left[u_0 - u_{mf}\right]^{0.4}.[z]^{0.8}.g^{-0.2} \quad (11)$$

The mean bubble diameter along the bed can be calculated by integrating Eq. (11) from $z = 0\ to\ z = H_{eb}$ as given below;

$$d_{bm} = 0.3\left[u_0 - u_{mf}\right]^{0.4}.[H_{eb}]^{0.8}.g^{-0.2} \quad (12)$$

Bubble Rise Velocity

For Bubbles in bubbling bed, the rise velocity is given by the following equation:

$$u_b = [u_0 - u_{mf}] + u_{br} \quad (13)$$

Where u_{br} is the rise velocity of a single bubble estimated using the expression reported by Kunii-Levenspiel [22] as follows,

$$u_{br} = 0.711\,[g\,d_b]^{0.5} \quad (14)$$

The effective gas velocity through the bubble phase can be defined from the gas balance in a cross section of the bed as follows;

$$u_b^* = \frac{u_0 - (1-\delta)u_{mf}}{\delta} \quad (15)$$

Bed Expansion

The fraction of bubble phase in the fluidized bed (δ) is proportional to the fluidization velocity of inlet gas. For intermediate bubbles, the following expression has been proposed by Abanades et al. [27]:

$$\delta = \frac{u_0 - u_{mf}}{u_b + \frac{5u_{mf} - u_b.\varepsilon_{mf}}{4}} \quad (16)$$

Also, expanded bed height is related to bubble fraction by the following equation;

$$H_{eb} = \frac{H_{mf}}{1-\delta} \quad (17)$$

It can be concluded from eqs. (12), (13), (14), (16), and (17), that an iterative solution is required to evaluate the expanded bed height, bubble size and velocity, and bubble fraction of the fluidized bed [28].

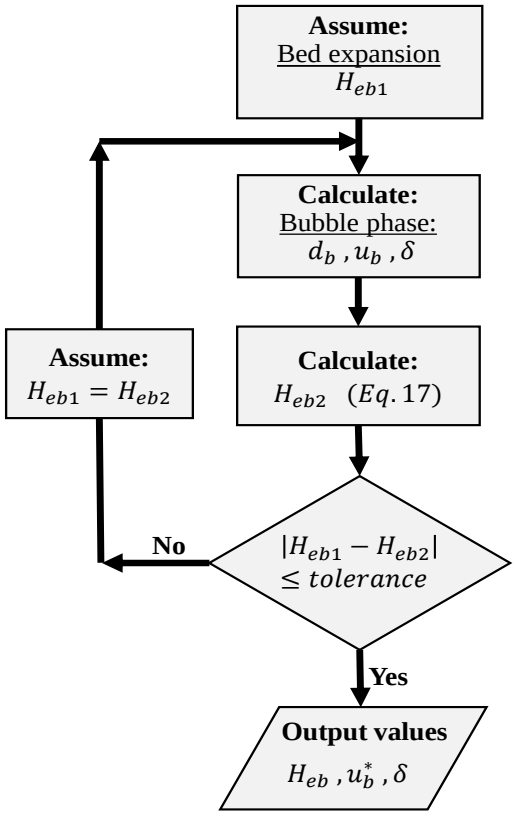

Fig. 3 Iterative calculation of hydrodynamic parameters

2.3 Reactor Model

Species conservation is applied on both phases of fluidized bed reactor. Assuming no accumulation of gas in control volume, the rate of outflow should equal the summation of rate of inflow, rate of mass transfer to the control volume and rate of generation by chemical reaction.

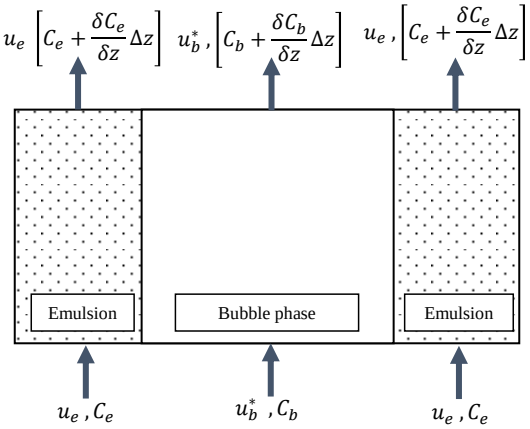

Fig. 4 Schematic of bubbling bed control volume

○ *For Emulsion phase,*

The conservation equation can be written as follows,

$$\left[C_e + \frac{\delta C_e}{\delta z}\Delta z\right].A_e.u_{mf} = C_e.A_e.u_{mf} + K_{be}[C_b - C_e].A_b.\Delta z - R_{CO_2}.A_e.\Delta z.\varepsilon_{mf} \quad (18)$$

Eq. (18) can be rearranged to give;

$$\frac{\delta C_e}{\delta z} = \frac{K_{be}}{u_{mf}}.\frac{\delta}{1-\delta}[C_b - C_e] - \frac{\varepsilon_{mf}}{u_{mf}}.R_{CO_2} \quad (19)$$

The last term in Eq. (19), (R_{CO_2}) is the rate of consumption of CO_2 due to chemical reaction; where,

$$R_{CO_2}\left[\frac{mol}{m^3_{gas}.s}\right] = \frac{1}{V_g}\frac{dN_{CO_2}}{dt} = \frac{1-\varepsilon_{mf}}{\varepsilon_{mf}} * \left(\frac{\rho_s}{MW_s}\frac{\delta X}{\delta t}\right) \quad (20)$$

○ *For Bubble phase,*

As bubbles are free of solid particles, therefore no chemical reaction takes place in the bubble phase. Conservation of carbon dioxide in bubble element can be written as:

$$\frac{\delta C_b}{\delta z} = -\frac{K_{be}}{u_b^*}\,[C_b - C_e] \quad (21)$$

The average conversion (or conversion ratio) (X_{avg}) of sorbent at any time can be calculated using the following expression:

$$X_{avg} = \frac{MW_s}{W_s} * Q_{gas,in} * \int_0^t \left[C_{CO_2,in} - C_{CO_2,out} * \frac{1-x_{CO_2,in}}{1-x_{CO_2,out}}\right] dt \quad (22)$$

A common performance parameter used in applications of carbon dioxide capture is the capture efficiency ($\eta_{capture}$). It is defined as the ratio between the number of moles of captured CO_2 to the number of moles of CO_2 entering the carbonator.

$$\eta_{capture} = \frac{N_{CO_2,Captured}}{N_{CO_2,Entering}} = 1 - \frac{C_{CO_2,out}}{C_{CO_2,in}} \quad (23)$$

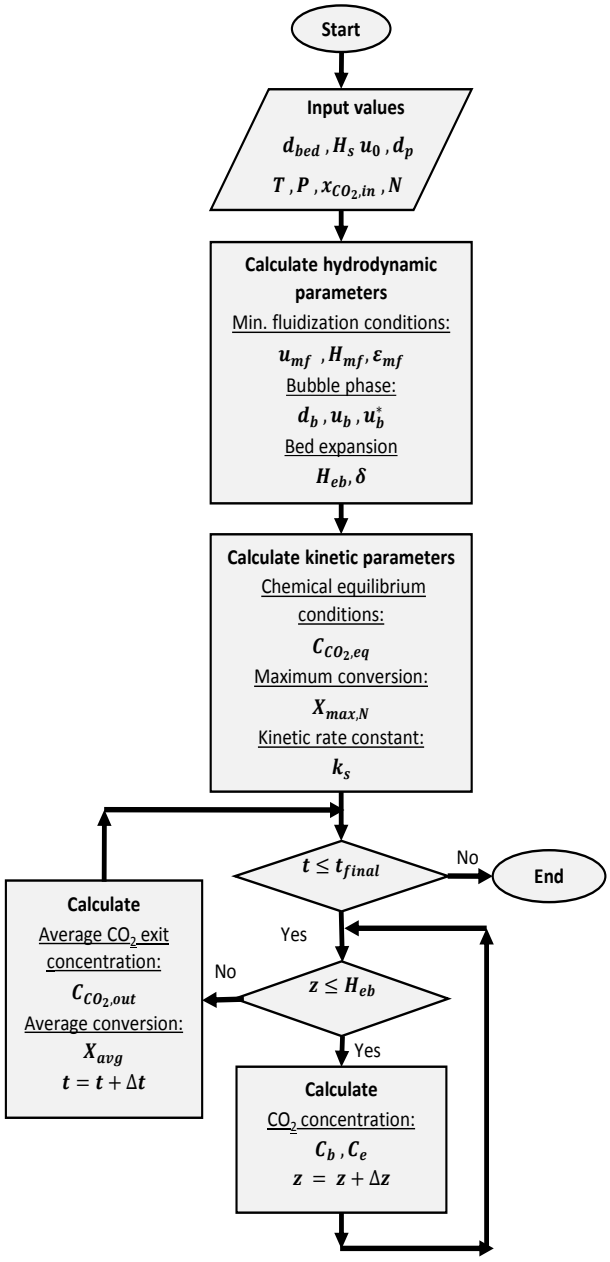

Fig. 5 Flowchart of the carbonator model

Numerical Solution

The carbonator model has been implemented in MATLAB 2014b [29]. Fig. 5 shows a flowchart of the algorithm used. After the introduction of the input values, the hydrodynamic and kinetic models are run to calculate the parameters required for eqs. (19), (20) and (21). Then, this system of equations is solved at each time step with the condition that ($at\ z = 0$, $C_b = C_e = C_{inlet}$) to give the average CO_2 exit concentration (C_{exit}). The rate of change of CO_2 concentration in emulsion is so rapid at the bottom of bed and then gets very slow. Solution of the system using fixed step methods would either lead to inaccuracy of results in case of using relatively large step size or high consumption of time and calculation power in case of using too small step size all over the bed. The use of adaptive step size method would solve this problem. The algorithm

used would reduce the step size (less than 0.1 mm) where the rate of change is high to spot this change accurately and relatively increase step size where the rate is low to save computational time and power.

III. RESULTS AND DISCUSSION

In this section, model outputs are presented at different operating conditions. The model is capable of predicting carbon dioxide mole fraction at any height and at any instance, Fig. 6. For illustration purposes, a fluidization column with inner diameter of 10.5 cm loaded with lime particles of static height of 15 cm operating at fluidization velocity of 0.8 m/s and temperature of 650 °C is considered. Inlet gas is composed of carbon dioxide and nitrogen with mole fractions of 15% and 85%, respectively. Fig. 7 shows CO_2 mole fraction vs. height after 10 minutes of operation calculated using the proposed model. It indicates that carbonation reaction taking place in emulsion phase is so rapid that CO_2 mole fraction in emulsion gas decreased from 15% to about 2% in less than two centimeters. After that, the calcium oxide is primarily reacting with the CO_2 transferred from bubbles to emulsion. Hence, optimization of mass transfer between bubble and emulsion phases would make significant improvements in the capturing process as indicated by Alabeedy et al. [30].

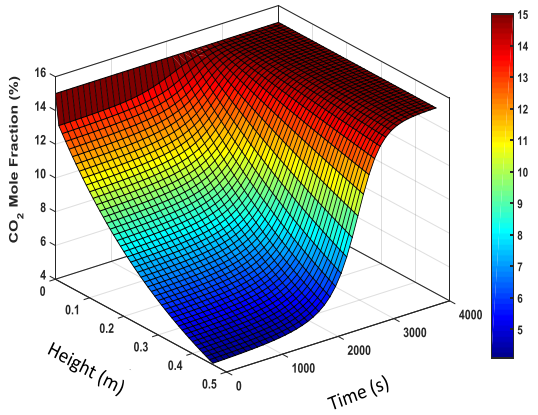

Fig. 6 Axial distribution of CO2 concentration with time at 650 °C

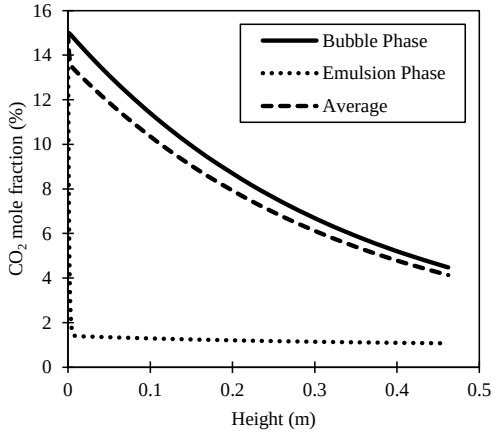

Fig. 7 Predicted CO2 mole fraction vs. height after 10 minutes at 650 °C

A. *Model Validation*

Results obtained using a mathematical model proposed by Abanades et al. [27] and experimental results from Alabeedy et al. [30] have been selected for validation purposes. Fig. 8 shows comparison between CO_2 mole fraction at the bed exit as predicted using the present study and the model propsed by Abanades et al. [27].

Experimental results from Alabeedy et al. [30] and model results of exit mole fraction of carbon dioxide, capture efficiency and conversion ratio versus time at a fluidization velocity of 0.8 m/s and bed temperature of 650 °C are shown in Fig. 9, Fig. 10 and Fig. 11. These comparisons indicate satisfying reliability of the proposed model.

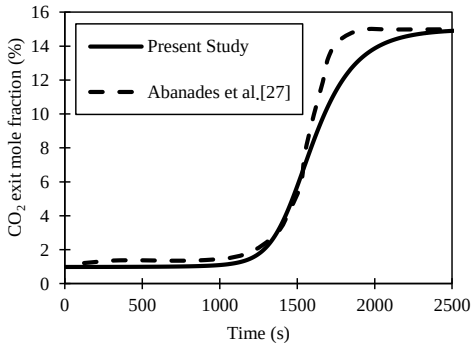

Fig. 8 Comparison between present study and Abanades et al. [27] (5 kg of Cadomin limestone, 650°C, u0 = 1m/s, 15 vol. % of CO2)

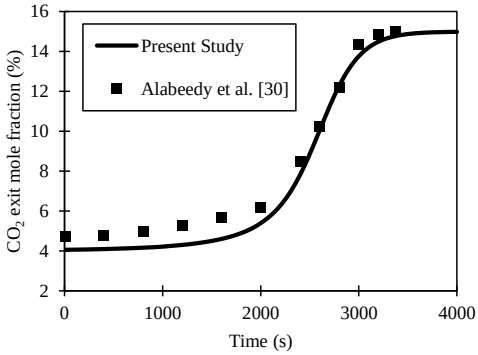

Fig. 9 CO2 exit mole fraction with time

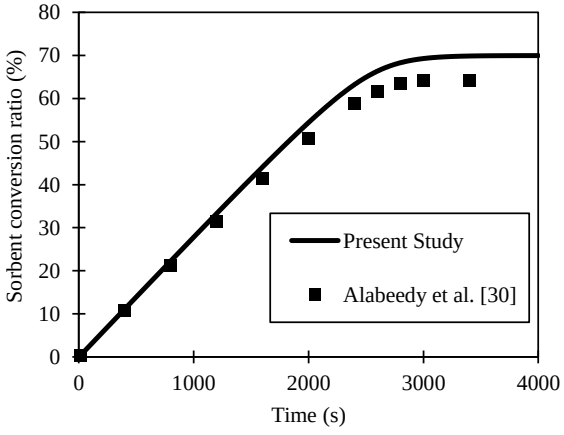

Fig. 10 Sorbent conversion ratio with time

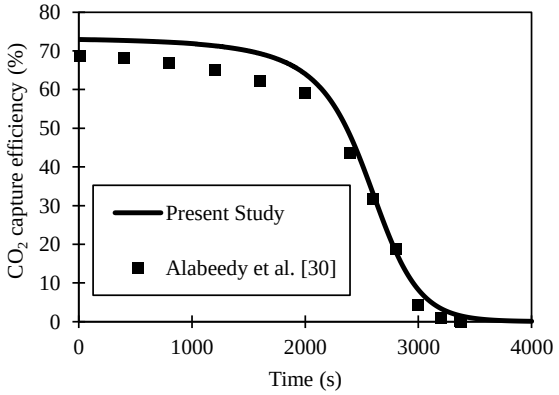

Fig. 11 CO2 capture efficiency with time

Parametric studies have been conducted to assess influences of operating parameters on carbonator behavior by evaluating capture efficiency at different bed temperatures, fluidization velocities, particle sizes, and static bed height.

B. Effect of Operating Temperature

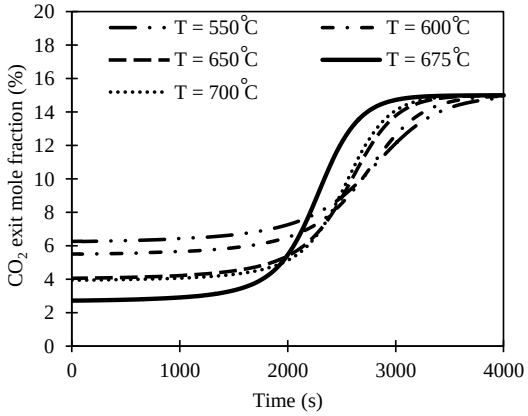

Fig. 12 CO2 exit mole fraction with time at different bed temperatures (u0=0.8 m/s)

Figure 12 shows the model results at different temperatures from 550 $°C$ to 700$°C$. The average capture efficiency versus bed temperature is shown in Fig. 13. The maximum average capture efficiency is found to occur around a bed temperature of 675 °C. To understand the existence of such optimum bed temperature, we need to keep in mind that operating temperature has two opposing effects. The positive effect is that increasing temperature enhances the chemical kinetics of the carbonation reaction (Eq. (7)) and the negative effect is that increasing temperature also increases the equilibrium concentration and partial pressure of carbon dioxide which slows down the reaction (Eq. (6)). From 550 °C to 675 °C, the chemical kinetic term is dominant leading to an increase in average efficiency and after that the increasing equilibrium concentration becomes more dominant resulting in a decrease in average efficiency. An optimum temperature of 675 °C has also been reported by Mostafavi et al. [31].

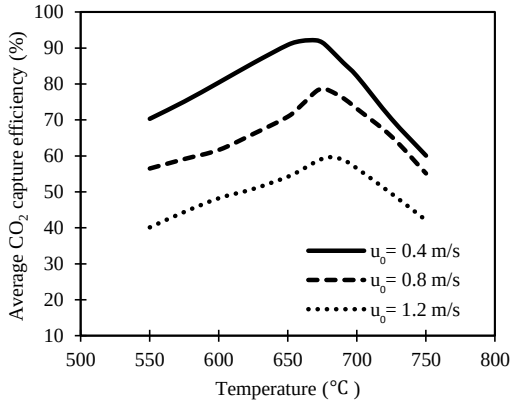

Fig. 13 Average CO2 capture efficiency vs. bed temperature

Figure 13 also indicates that decreasing fluidization velocity moves the peak slightly to the left. As fluidization velocity decreases, the gas molecules have increased residence time in the bed (i.e. have more time to react with solid sorbent) which reduces the effect of decreased reaction rate constant at lower temperatures.

C. Effect of Fluidization Velocity

Different fluidization velocities have been tested (from 0.4 to 1.2 m/s) to investigate the effect of hydrodynamics on the reactor, as shown in Fig. 14 and Fig. 15. Results indicate that the average efficiency increases with decreasing the fluidizing velocity due to increased residence time and enhanced mass transfer from bubbles to emulsion. Similar results were reported by [30]. However decreasing inlet velocity would require a wider reactor (or even more than one reactor) to handle the required flow rate of flue gases. So a compromise between performance and capital cost would be required.

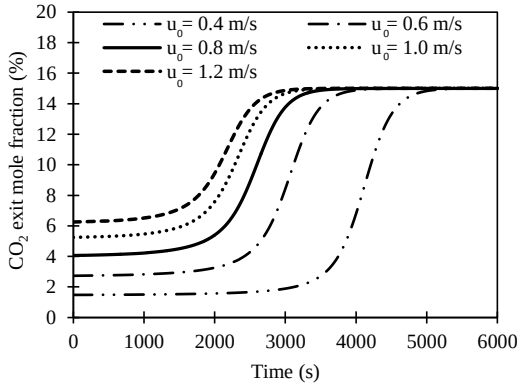

Fig. 14 CO2 exit mole fraction with time at different fluidization velocities (T=650 °C).

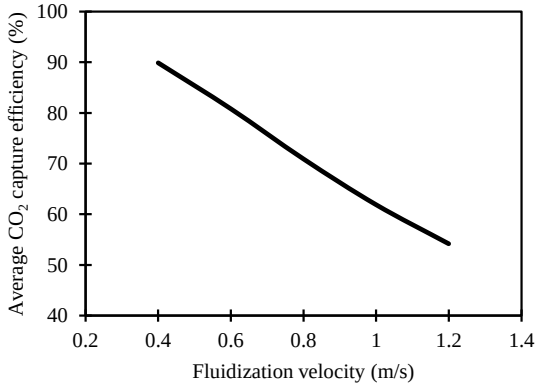

Fig. 15 Average CO2 capture efficiency vs. fluidization velocity (at T=650 °C).

D. *Effect of Bed Particle Size*

Increasing particle size was found to result in a decrease in exit CO_2 mole fraction and an increase in the capture efficiency of the carbonator as shown in Fig. 16 and Fig. 17. It should be noted that increasing particle size results in an increase in minimum fluidization velocity. Consequently larger particles lead to less bubbling bed as long as the fluidization velocity is kept constant. This is analogous to decreasing fluidization velocity with the same particle size as discussed above. However, changing particle size is expected to change the porous structure of solid reactant leading to a change in kinetic parameters. Although Bhatia and Perlmutter [32] reported negligible effect of particle size on the kinetic parameters, more investigations on the porous structure of lime particles is required to fully describe the dependency of capture efficiency on particles size.

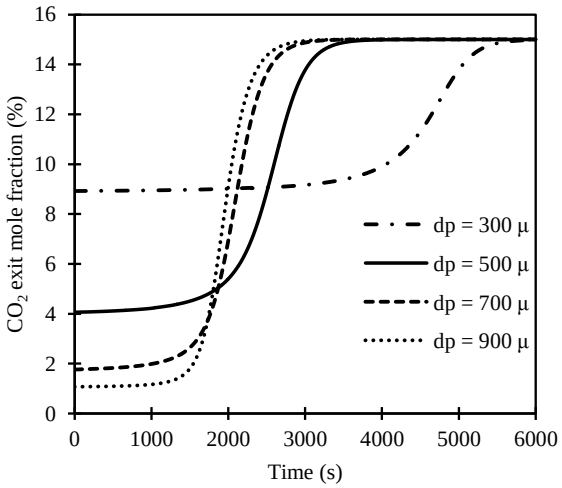

Fig. 16 CO2 Exit mole fraction with time at different particles sizes (T=650 °C, u0=0.8 m/s).

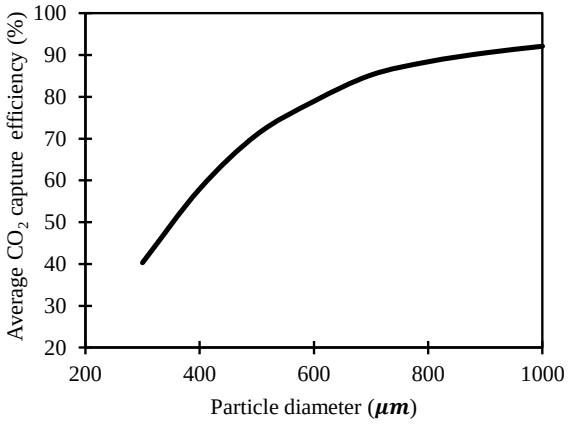

Fig. 17 Average CO2 capture efficiency vs. particle diameter (T=650 °C, u0=0.8 m/s).

E. *Effect of Static Bed Height*

In order to understand the effects of static bed height on carbon dioxide capture, the model has been run at different heights (from 0.05 m to 0.90 m). Fig. 18 shows model prediction for the mole fraction of carbon dioxide at the exit of reactor. Increasing bed height increases carbonation time due to increasing active solid inventory. Also, reaction is allowed to proceed longer and flue gases get in contact with active particles for more time as they pass through the bed which improves the capture efficiency. However, Fig. 19 shows that further increase of bed height has little effect on capture efficiency improvement. This is due to the fact that bubbles continue to expand and coalesce with height, so the higher zones of the bed suffer from poor mass transfer coefficient and probably the bed turns into slugging.

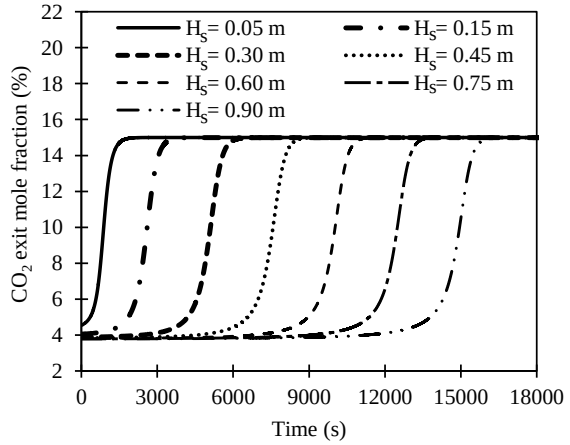

Fig. 18 CO2 exit mole fraction with time at different bed heights (T=650 °C, u0=0.8 m/s)

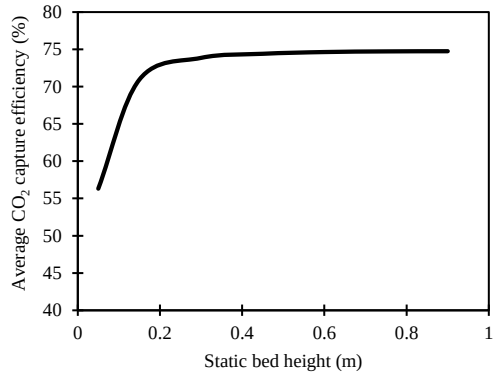

Fig. 19 Average CO2 capture efficiency vs. static bed height (T=650 °C, u0=0.8 m/s).

IV. CONCLUSION

A dynamic model has been presented to evaluate carbon dioxide capture using the carbonation reaction between calcium oxide (from lime) and carbon dioxide. It describes carbonator performance at different conditions. The model makes a coupling between hydrodynamics and kinetics to give more realistic insights. It can be used to make design choices such as bed sizing and determine optimum operating conditions that maximize the capture efficiency. Carbonator model can be integrated with the whole plant simulations to predict thermal efficiency penalties of the carbon capture process.

The dependency of performance on different input parameters has been discussed. Operating temperature has major effects as it determines kinetic constants and equilibrium conditions. Fluidization velocity determines the residence time and mass transfer coefficients. An increase in particles size affects minimum fluidization conditions and causes the bed to be less bubbling with better mass transfer. However further investigations on the effect of particle size on kinetic constants are required. Static Bed height has little effects on the capture efficiency except at relatively low heights.

V. NOMENCLATURE

Symbol Description

A_b	Cross sectional area of bubble phase, m^2
A_e	Cross sectional area of emulsion phase, m^2
Ar	Archimedes number
C_b	Gas molar concentration in bubble phase, mol/m^3
C_e	Gas molar concentration in emulsion phase, mol/m^3
C_{CO2}	CO_2 molar concentration, mol/m^3
C_{CO2},eq	CO_2 molar concentration at equilibrium, mol/m^3
$C_{CO2,in}$	CO_2 molar concentration at bed inlet, mol/m^3
$C_{CO2,out}$	CO_2 molar concentration at bed outlet, mol/m^3
d_b	Bubble diameter, m
d_{bm}	Mean bubble diameter, m
d_p	Particle diameter, m
E	Reaction activation energy, J/mol
g	Gravitational acceleration, m/s^2
H_{eb}	Expanded bed height, m
H_{mf}	Bed height at minimum fluidization, m
H_s	Static bed height, m
K_{be}	Mass interchange coefficient between bubble and emulsion phase, s^{-1}
k_0	Pre-exponential factor in Eq. (7), $mol.Pa^{(-n)}/m^2.s$
k_s	Intrinsic surface rate constant, $mol.Pa^{(-n)}/m^2.s$
MW_s	Molecular weight of solid,kg/mol
N	Number of calcination/ carbonation cycles
n	Order of reaction
P_{CO2}	CO_2 partial pressure, Pa
$P_{CO2,eq}$	CO_2 partial pressure at equilibrium, Pa
$Q_{gas,in}$	Volumetric flow rate of flue gases at bed inlet, m^3/s
R	Specific reaction rate, s^{-1}
R_{CO_2}	Rate of consumption of CO_2, $mol/m^3_{gas}.s$
R_u	Universal gas constant, J/mol.K
$Re_{p,mf}$	Reynolds number at minimum fluidization
r	Grain radius at any time, m
r_0	Initial grain radius, m
S	Surface area of solid particles at any time, m^2/g
S_0	Initial surface area of solid particles, m^2/g
T	Operating temperature, K
t	Time, s
u_0	Fluidization velocity, m/s
u_b	Rise velocity of bubble phase,m/s
u_b^*	The effective gas velocity through the bubble phase, m/s
u_{bm}	Mean rise velocity of bubble phase, m/s
u_{br}	Rise velocity of single bubble,m/s
u_e	Rise velocity of emulsion gas,m/s
u_{mf}	Minimum fluidization velocity, m/s
V_g	Volume of gas in the control volume, m^3
W_s	Mass of solid sorbent in bed, kg
X	Conversion ratio of solid sorbent
X_{avg}	Average conversion ratio of solid sorbent
$X_{max,N}$	Maximum sorbent capacity after N cycles
$x_{CO_2,in}$	Carbon dioxide mole fraction at bed inlet
$x_{CO_2,out}$	Carbon dioxide mole fraction at bed outlet
z	Axial distance measured from air distributor, m

Greek Symbols

ε_{mf}	Bed voidage fraction at minimum fluidization
ρ_g	Gas density, kg/m^3
ρ_s	Solid particles density, kg/m^3
δ	The fraction of bed consisting of bubbles
μ	Dynamic viscosity, $N.s/m^2$
ϕ	Solid particles sphericity
$\eta_{capture}$	CO_2 capture efficiency

REFERENCES

[1] B. Metz, O. Davidson, H. C. De Coninck, M. Loos, and L. A. Meyer, "IPCC, 2005: IPCC special report on carbon dioxide capture and storage. Prepared by Working Group III of the Intergovernmental Panel on Climate Change," *Cambridge, United Kingdom New York, NY, USA*, vol. 442, 2005.

[2] M. E. Boot-Handford, J. C. Abanades, E. J. Anthony, M. J. Blunt, S. Brandani, N. Mac Dowell, J. R. Fernández, M.-C. Ferrari, R. Gross, J. P. Hallett, R. S. Haszeldine, P. Heptonstall, A. Lyngfelt, Z. Makuch, E. Mangano, R. T. J. Porter, M. Pourkashanian, G. T. Rochelle, N. Shah, J. G. Yao, and P. S. Fennell, "Carbon capture and storage update," *Energy Environ. Sci.*, vol. 7, no. 1, pp. 130–189, 2014.

[3] J. C. Abanades, B. Arias, A. Lyngfelt, T. Mattisson, D. E. Wiley, H. Li, M. T. Ho, E. Mangano, and S. Brandani, "Emerging CO_2 capture

systems," *International Journal of Greenhouse Gas Control*, vol. 40, no. May. pp. 126–166, 2015.

[4] T. Hirama, H. Hosoda, K. Kunihiro, and T. Shimizu, "Separating carbon dioxide from gases containig it." UK Patent, 1996.

[5] T. Shimizu, T. Hirama, H. Hosoda, K. Kitano, M. Inagaki, and K. Tejima, "A Twin Fluid-Bed Reactor for Removal of CO_2 from Combustion Processes," *Chem. Eng. Res. Des.*, vol. 77, no. 1, pp. 62–68, 1999.

[6] J. C. Abanades, E. J. Anthony, J. Wang, and J. E. Oakey, "Fluidized Bed Combustion Systems Integrating CO_2 Capture with CaO," *Environ. Sci. Technol.*, vol. 39, no. 8, pp. 2861–2866, Apr. 2005.

[7] B. R. Stanmore and P. Gilot, "Review-calcination and carbonation of limestone during thermal cycling for CO_2 sequestration," *Fuel Process. Technol.*, vol. 86, no. 16, pp. 1707–1743, 2005.

[8] C. C. Dean, J. Blamey, N. H. Florin, M. J. Al-Jeboori, and P. S. Fennell, "The calcium looping cycle for CO_2 capture from power generation, cement manufacture and hydrogen production," *Chem. Eng. Res. Des.*, vol. 89, no. 6, pp. 836–855, Jun. 2011.

[9] D. Y. Lu, R. W. Hughes, and E. J. Anthony, "Ca-based sorbent looping combustion for CO_2 capture in pilot-scale dual fluidized beds," *Fuel Process. Technol.*, vol. 89, no. 12, pp. 1386–1395, 2008.

[10] W. Wang, S. Ramkumar, S. Li, D. Wong, M. Iyer, B. B. Sakadjian, R. M. Statnick, and L.-S. Fan, "Subpilot Demonstration of the Carbonation−Calcination Reaction (CCR) Process: High-Temperature CO_2 and Sulfur Capture from Coal-Fired Power Plants," *Ind. Eng. Chem. Res.*, vol. 49, no. 11, pp. 5094–5101, Jun. 2010.

[11] B. Arias, M. E. Diego, J. C. Abanades, M. Lorenzo, L. Diaz, D. Martínez, J. Alvarez, and A. Sánchez-Biezma, "Demonstration of steady state CO_2 capture in a 1.7MWth calcium looping pilot," *Int. J. Greenh. Gas Control*, vol. 18, pp. 237–245, Oct. 2013.

[12] A. Charitos, N. Rodríguez, C. Hawthorne, M. Alonso, M. Zieba, B. Arias, G. Kopanakis, G. Scheffknecht, and J. C. Abanades, "Experimental Validation of the Calcium Looping CO_2 Capture Process with Two Circulating Fluidized Bed Carbonator Reactors," *Ind. Eng. Chem. Res.*, vol. 50, no. 16, pp. 9685–9695, Aug. 2011.

[13] E. H. Baker, "The Calcium Oxide-Carbon Dioxide System in the Pressure Range 1-300 Atmospheres," *J. Chem. Inf. Model.*, pp. 464–470, 1962.

[14] D. Alvarez and J. C. Abanades, "Determination of the Critical Product Layer Thickness in the Reaction of CaO with CO_2," *Ind. Eng. Chem. Res.*, vol. 44, no. 15, pp. 5608–5615, Jul. 2005.

[15] M. Alonso, N. Rodríguez, G. Grasa, and J. C. Abanades, "Modelling of a fluidized bed carbonator reactor to capture CO_2 from a combustion flue gas," *Chem. Eng. Sci.*, vol. 64, no. 5, pp. 883–891, 2009.

[16] M. C. Romano, "Modeling the carbonator of a Ca-looping process for CO_2 capture from power plant flue gas," *Chem. Eng. Sci.*, vol. 69, no. 1, pp. 257–269, 2012.

[17] Z. Li, F. Fang, X. Tang, and N. Cai, "Effect of Temperature on the Carbonation Reaction of CaO with CO_2," 2012.

[18] J. Szekely and J. W. Evans, "GAS-SOLID REACTIONS," 1976.

[19] P. Sun, J. R. Grace, C. J. Lim, and E. J. Anthony, "Determination of intrinsic rate constants of the CaO-CO_2 reaction," *Chem. Eng. Sci.*, vol. 63, no. 1, pp. 47–56, 2008.

[20] R. Barker, "The reversibility of the reaction $CaCO_3 \rightleftarrows CaO + CO_2$, *J. Appl. Chem. Biotechnol.*, vol. 23, no. 10, pp. 733–742, 1973.

[21] G. S. Grasa and J. C. Abanades, "CO_2 Capture Capacity of CaO in Long Series of Carbonation / Calcination Cycles," pp. 8846–8851, 2006.

[22] D. Kunii and O. Levenspiel, *Fluidization Engineering*. 1991.

[23] C. Y. Wen and Y. H. Yu, "A generalized method for predicting the minimum fluidization velocity," *AIChE J.*, vol. 12, no. 3, pp. 610–612, 1966.

[24] J. R. Grace, "Contacting modes and behaviour classification of gas—solid and other two-phase suspensions," *Can. J. Chem. Eng.*, vol. 64, no. 3, pp. 353–363, 1986.

[25] T. E. Broadhurst and H. A. Becker, "Onset of fluidization and slugging in beds of uniform particles," *AIChE J.*, vol. 21, no. 2, pp. 238–247, 1975.

[26] R. C. Darton, R. D. LaNauze, J. F. Davidson, and D. Harrison, "Bubble growth due to coalesence in fluidised beds," *Trans Inst Chem Eng*, vol. 55, no. 4, pp. 274–280, 1977.

[27] J. C. Abanades, E. J. Anthony, D. Y. Lu, C. Salvador, and D. Alvarez, "Capture of CO_2 from combustion gases in a fluidized bed of CaO," *AIChE J.*, vol. 50, no. 7, pp. 1614–1622, Jul. 2004.

[28] F. Okasha, "Modeling of liquid fuel combustion in fluidized bed," *Fuel*, vol. 86, no. 15, pp. 2241–2253, 2007.

[29] The MathWorks Inc, "MATLAB 2014b." Natick, Massachusetts, United States, 2014.

[30] A. A. Alabeedy, A. A. Hegazi, and F. Okasha, "Enhancing Carbonation Process during Carbon Dioxide Capturing Applying Jetting Fountain Fluidized Bed," *Mansoura Eng. J.*, vol. 41, no. 1, 2016.

[31] E. Mostafavi, M. H. Sedghkerdar, and N. Mahinpey, "Thermodynamic and Kinetic Study of CO_2 Capture with Calcium Based Sorbents: Experiments and Modeling," *Ind. Eng. Chem. Res.*, vol. 52, no. 13, pp. 4725–4733, 2013.

[32] S. K. Bhatia and D. D. Perlmutter, "Effect of the product layer on the kinetics of the CO_2-lime reaction," *AIChE J.*, vol. 29, no. 1, pp. 79–86, 1983.